

Ultrastructural Alteration of Osteoclasts Treated with Brefeldin A and Wortmannin

Naoya Izumi¹, Norio Amizuka¹, Kimimitsu Oda², Yoshio Misumi³, Yukio Ikehara³ and Hidehiro Ozawa¹

¹First Department of Oral Anatomy and ²Department of Oral Biochemistry, Niigata University Faculty of Dentistry, 5274, 2-Bancho, Gakkoucho-Dori, Niigata 951-8514 and ³Second Department of Biochemistry, Fukuoka University School of Medicine, 7-45-1, Nanakuma, Jonan-Ku, Fukuoka 814-0133

Received January 18, 1999; accepted September 20, 1999

Osteoclasts secrete protons and lysosomal enzymes through ruffled borders, resulting in demineralization and degradation of bone matrix. Golgi apparatus is thought to play a key role in this process. In order to elucidate the specific functions of Golgi apparatus in osteoclasts, we observed the ultrastructural and cytochemical changes resulting from the administration of brefeldin A (BFA), an inhibitor of Golgi structures, and wortmannin (WT), an inhibitor of phosphatidylinositol 3-kinase (PI3-kinase). When treated with BFA, osteoclasts showed a dissociated Golgi apparatus, while the peanut agglutinin (PNA)-positive ruffled borders were poorly developed or disappeared. Moreover, the

acid phosphatase (ACPase) activity was somewhat reduced. WT-treated osteoclasts, on the other hand, exhibited no ultrastructural alteration of the Golgi apparatus, but were marked by the disappearance of PNA-positive ruffled borders, and a consequent increase in the number of ACPase-positive vesicles and vacuoles in the cytoplasm. These results indicate that the Golgi apparatus of osteoclasts not only plays an important role in the formation of lysosomal enzymes but also the supply of ruffled border membranes. Furthermore, PI 3-kinase appears to be involved in the transport of lysosomal enzymes and the maintenance of ruffled borders.

Key words: Osteoclast, Brefeldin A, Wortmannin, Golgi apparatus, Ruffled border

I. Introduction

Multinucleated osteoclasts secrete protons through ruffled borders, resulting in demineralization of bone matrix [4, 33], and degrade organic components of bone matrix by secreting several osteolytic enzymes, such as acid phosphatase (ACPase) [1, 23, 28, 29, 39], cysteine proteinases [16, 26] and matrix metalloproteinase [41, 47].

Golgi apparatus plays a key role in intracellular function, especially the sorting and targeting of newly-synthesized proteins, that are destined for cell-surfaces as well as lysosomes, and extracellular secretion [17]. Therefore, the Golgi apparatus in osteoclasts is thought to take part in the modification, sorting and secretion of osteolytic enzymes. Cameron [7] has demonstrated that the Golgi apparatus of osteoclasts is composed of several groups of

flattened sacs at intervals around the nuclei. The sacs were layered together with clusters of small vesicles adjacent to each group. Some vesicles in the Golgi region contained crystals, while others possessed material of a density comparable to that of vesicles nearby, or in other parts of the cytoplasm, where they lie among larger vesicles derived from the ruffled border. Dense material was also found in tubular or canalicular structures that extended from near the Golgi membranes to the ruffled border. There were also larger dense bodies distributed in a similar manner, that may belong to the lysosome family. Cytochemical investigations revealed lysosomal enzymes, such as ACPase [1, 23, 28, 36] and arylsulfatase [2, 3] to localize in the Golgi apparatus of osteoclasts. Furthermore, alpha-2,6-sialyltransferase, a trans-Golgi marker enzyme, was present in each stack of Golgi cisternae, but limited to just those one or two cisternae that were located in trans site, thereby demonstrating that the Golgi apparatus in the osteoclasts was functionally compartmentalized [3]. Lectin cytochemistry showed

Correspondence to: Hidehiro Ozawa, D. D. S., PhD, First Department of Oral Anatomy, Niigata University Faculty of Dentistry, 5274, 2-Bancho, Gakkoucho-Dori, Niigata 951-8514, Japan.

that concanavalin A, *Maclura pomifera* agglutinin and wheat germ agglutinin reacted in the Golgi apparatus in the osteoclast, suggesting that glycosylation occurred there [32, 45]. There are many reports about ultrastructural and cytochemical aspects of the Golgi apparatus of osteoclasts, but it is unclear how morphological changes of the Golgi apparatus affect the bone resorption mechanism of osteoclasts.

Brefeldin A (BFA), one of the fungal metabolites, has been shown to impede protein transport from rough endoplasmic reticulum (rER) to Golgi apparatus, thereby halting protein secretion *in vitro* [31, 38]. It has also been shown that BFA caused a rapid disassembly of the Golgi apparatus and redistribution of the Golgi-localized proteins into the rER [13, 14, 24, 25]. Therefore, the specific biochemical function of BFA can be of great benefit in investigating the intracellular vesicular traffic associated with Golgi apparatus. On the other hand, wortmannin (WT), a specific inhibitor of phosphatidylinositol-3 kinase (PI3-kinase) [40, 49], has been implicated in the regulation of membrane traffic. It has been reported that inhibition of PI3-kinase with WT resulted in the missorting of newly synthesized lysosomal enzymes [6, 8]. This inhibitor not only reduced bone resorption [18, 35], but caused the disappearance of ruffled borders [34, 35] in osteoclasts, *in vitro*.

In order to clarify the correlation between morphological changes of Golgi apparatus and cellular functions of osteoclasts, especially with regard to the structure of ruffled borders, we observed the BFA- or WT-treated osteoclasts in rat tibiae, *in vivo*. As part of our investigation of the distribution of the Golgi apparatus in osteoclasts, we examined the immunolocalization of rat 364-kD Golgi-associated protein (GCP364), which may be involved in the formation and/or maintenance of the Golgi structure [48], using confocal laser scanning microscope (CLSM). We then noted the ultrastructural changes that took place in the Golgi apparatus and other cell organelles, when treated with BFA or WT, employing transmission electron microscope (TEM). In addition, the altered localization of ACPase, which has been known to localize in trans-cisternae of Golgi apparatus, trans-Golgi network (TGN), lysosomes [12] and ruffled borders in osteoclasts [1, 23, 28, 29, 39] was investigated, using enzyme cytochemical procedures. For elucidation of the morphological changes of ruffled borders in the BFA- or WT-treated osteoclasts, we have examined peanut agglutinin (PNA)-reactivity, since PNA has been reported to recognize terminal β -D-galactose-(1-3)-N-acetyl-D-galactosamine residues [27] and to bind the ruffled border membranes of osteoclasts [32, 45]. Using the histological techniques described above, we have assessed the specific functions of Golgi apparatus in osteoclasts.

II. Materials and Methods

Tissue preparation

Three-week-old male Wistar rats (Nihon SLC, Hamamatsu, Japan) weighing approximately 60 g were used in this experiment. BFA (Wako Pure Chemical Co., Osaka, Japan) was kept in a stock solution of 1 mg/ml in methanol at -80°C . Rats were anesthetized with Nembutal and intravenously injected with BFA. We have employed 2mg/kg of BFA dissolved in 10% methanol, which is twice as much as Misumi *et al.* have used [31]. Control animals were injected with 10% methanol lacking the BFA.

WT (Wako Pure Chemical Co., Osaka, Japan) was kept in a stock solution of 0.5 mg/ml in dimethyl sulfoxide (DMSO) at -20°C . In the experimental group, rats were anesthetized with Nembutal, and intravenously injected with 0.1 mg/kg WT dissolved in 2% DMSO, which is twice as much as Nakamura *et al.* have employed [35]. For a control experiment, the rats were injected with 2% DMSO without WT.

All animals were anesthetized and sacrificed at 30 min after the injection of BFA or WT. This period was most effective to bring about the morphological changes of osteoclasts by BFA or WT in this study.

Immunocytochemical study

The animals treated with the BFA or WT solution were anesthetized with Nembutal and perfused through the left ventricle, first with Ringer's solution, then with 4% paraformaldehyde in 0.05 M sodium cacodylate buffer (pH 7.4) for 10 min. The tibiae were dissected, immersed in the same fixative for 2 hr at 4°C and decalcified in 4.13% EDTA (pH 7.4) for 7 days at 4°C . Histological sections approximately 50 μm thick were obtained with a Microslicer DTK-1000 (D. S. K., Kyoto, Japan). After treatment with 0.5% Triton X-100 in phosphate buffered saline (PBS) for 30 min at room temperature, these sections were preincubated in 1% bovine serum albumin in PBS, for 1 hr at room temperature in order to prevent non-specific binding, and then, incubated with rabbit anti-recombinant rat 364-kD Golgi-associated protein (GCP364) antibodies [48] diluted to 1:200 for 48 hr at 4°C . After washing with PBS, they were incubated with FITC-conjugated goat anti-rabbit IgG (Cappel, Durham, NC, UK) diluted to 1:100 for 24 hr at 4°C , washed with PBS and examined under a confocal laser scanning microscope (CLSM, Olympus, LSM-GB 200, Tokyo, Japan). Negative control sections were incubated with normal rabbit serum in place of the primary antibodies.

Ultrastructural observations

After perfusion with a mixture of 2% paraformaldehyde and 2.5% glutaraldehyde, in 0.05 M sodium cacodylate buffer (pH 7.4), and immersion in the same fixative for 12 hr at 4°C , specimens were decalcified as per the above method. They were then postfixed with 1% osmium

tetroxide in 0.1 M sodium cacodylate buffer containing 1.5% potassium ferrocyanide for 2 hr at 4°C. They were dehydrated in a graded ethanol series and embedded in Poly/Bed 812 (Polyscience, Warrington, PA). Ultrathin sections were obtained by a Porter-Blum MT-1, and then, mounted on copper grids. They were stained with uranyl acetate and lead citrate, prior to observation under JEM-100CXII electron microscope (JEOL Ltd., Tokyo, Japan), at an accelerating voltage of 80 kV.

Detection of acid phosphatase

For ACPase enzyme-cytochemical observation, the rats were perfused with a mixture of 4% paraformaldehyde and 0.5% glutaraldehyde in 0.05 M sodium cacodylate buffer (pH 7.4), and then, immersed in the same fixative for 2 hr at 4°C prior to decalcification. For light microscopic observation, some specimens were dehydrated with an increasing concentration of ethanol and were embedded in paraffin. 5 μ m-thick sections were obtained using a sliding microtome. Dewaxed paraffin sections were incubated with a mixture of 5 mg naphthol AS-BI phosphate (Sigma, St. Louis, MO) as a substrate and 18 mg of red violet LB salt (Sigma) diluted in 30 ml 0.1 M acetate buffer (pH 5.0) at room temperature for 30 min. The sections were faintly counterstained with methyl green. For electron microscopic observation, the sliced sections approximately 50 μ m thick obtained with the Microslicer were incubated with a mixture of 5 ml 3% beta-glycerophosphate (Wako Pure Chemical Co., Osaka, Japan) as a substrate, 4 g of sucrose and 50 mg of lead nitrate (Nacalai tesque, INC., Kyoto, Japan) diluted in 50 ml of 0.05 M acetate buffer (pH 5.0) at room temperature for 30 min [15]. Following incubation, the sections were postfixed with 1% osmium tetroxide in 0.1 M sodium cacodylate buffer containing 1.5% potassium ferrocyanide for 1 hr at 4°C and embedded in Poly/Bed 812 for TEM observation.

PNA lectin cytochemistry

For this segment of cytochemical studies, the rats were perfused with a mixture of 2% paraformaldehyde and 2.5% glutaraldehyde in 0.05 M sodium cacodylate buffer (pH 7.4), and were immersed in the same fixative for 2 hr at 4°C. The sliced sections approximately 50 μ m thick obtained with the Microslicer were incubated in PBS containing horseradish peroxidase (HRP)-conjugated peanut agglutinin (PNA, Seikagaku Kogyo Co., Ltd. Tokyo, Japan) at a concentration of 20 μ g/ml for 24 hr, at 4°C. They were then washed with PBS, and were refixed with 2.5% glutaraldehyde in PBS. Following rinsing with PBS, they were immersed in DAB-H₂O₂ solution (0.05% Diaminobenzidine and 0.01% H₂O₂ in 0.05 M Tris-HCl buffer, pH 7.6) for 10 min, at room temperature, and postfixed with 1% osmium tetroxide in 0.1 M sodium cacodylate buffer for 1 hr at 4°C. They were dehydrated in a graded ethanol series and embedded in Poly/Bed 812 [32]. 1 μ m sections of Poly/Bed-embedded specimens

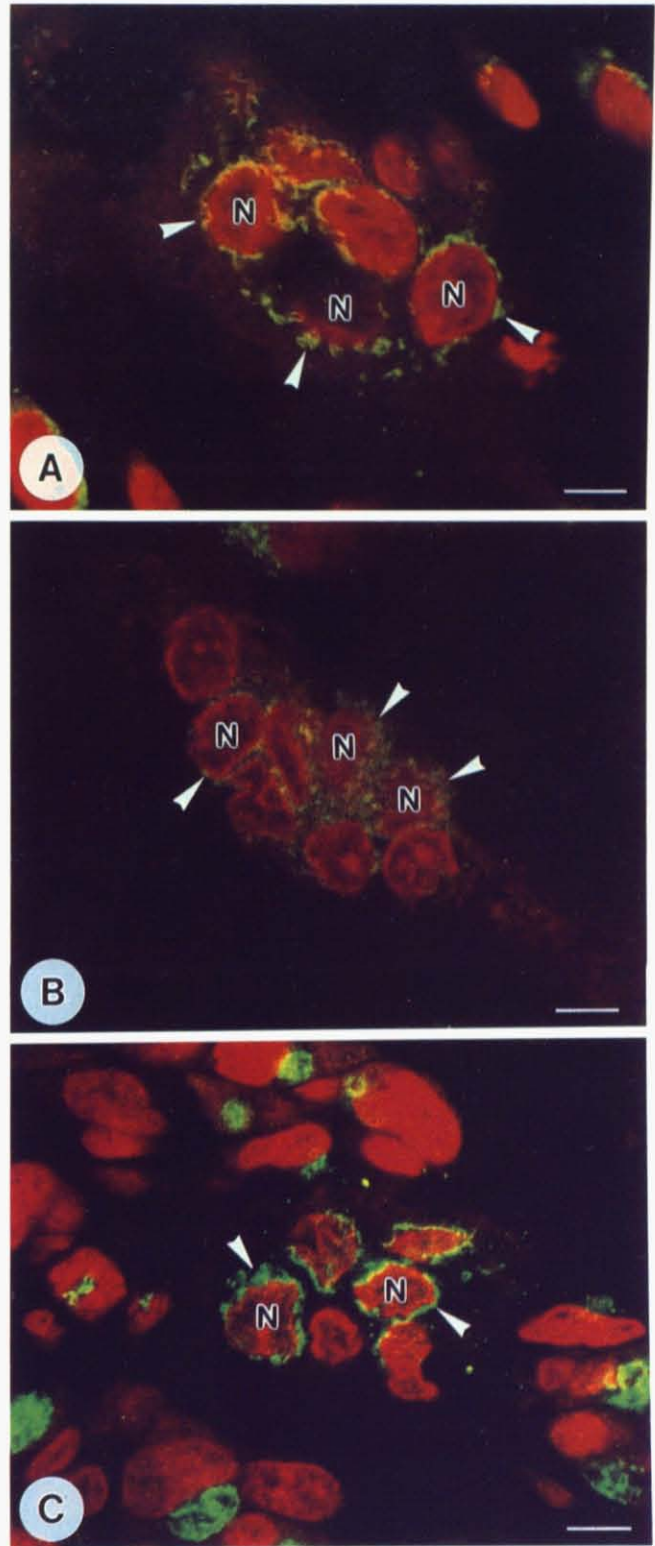


Fig. 1. Confocal laser scanning microscopic (CLSM) images showing the immunolocalization of GCP364 in osteoclasts. **A:** Control osteoclast. Immunoreactivity for GCP364 (arrowheads) is localized in the periphery of each nucleus (N). **B:** BFA-treated osteoclast. Low-level immunoreactivity for GCP364 (arrowheads) is detected in the vicinity of the nuclei (N). **C:** WT-treated osteoclast. Immunoreactivity for GCP364 (arrowheads) is localized in the periphery of each nucleus (N). The immunolocalization is identical to that in control osteoclasts. Original magnification = $\times 3000$, bar = 3 μ m.

were observed by light microscopy after counterstaining with toluidine blue. Furthermore, obtained ultrathin sections were observed under the TEM. As a control experiment, parts of sections were immersed in DAB-H₂O₂ solution without incubation in HRP-conjugated PNA.

Statistical analysis of osteoclasts which possess PNA-positive ruffled borders

Quantitative assessment was performed by counting PNA-positive osteoclasts in the area between 2.5 mm from the chondro-osseous junction and the diaphysis surrounded by cortical bones on both sides. Histological sections performed by PNA-lectin of tibiae of control, BFA-administered and WT-administered animals were examined (n=20). The percentage of the PNA-positive osteoclasts was represented by dividing by the total number of osteoclasts. Statistical analysis was performed by the Student's t-test. Osteoclasts were identified as giant cells possessing more than 2 nuclei.

III. Results

Immunocytochemical localization of GCP364

In order to elucidate the intracellular distribution of Golgi apparatus in osteoclasts treated with BFA or WT, we observed the immunolocalization of GCP364 under CLSM. GCP364-immunoreactivity was demonstrated in the periphery of each nucleus of the control osteoclast (Fig. 1A). After the administration of BFA, the images revealed the dispersed immunoreactivity for GCP364 in the vicinity of each nucleus (Fig. 1B), whereas, in WT-treated osteoclasts, the GCP364 immunolocalization was no different from that of controls (Fig. 1C).

No specific immunoreactivity was evident in those control sections which were incubated with normal rabbit serum.

Ultrastructural observations

Under TEM observation, control osteoclasts revealed well-developed ruffled borders adjacent to the bone surface, these ruffled borders being surrounded by clear zones (Fig. 2A). Fully-developed Golgi apparatus surrounded each nucleus of the osteoclasts. Abundant vesicles and vacuoles were detected between the Golgi apparatus and ruffled borders. Well-extended, but scattered rER could be seen throughout the cytoplasm. At a higher magnification, well-developed Golgi apparatus composed of both parallel arrays of three to four cisternae and many

vesicles adjacent to these cisternae were observed (Fig. 4A). Many vesicles were also observed around the trans-face and some cisternae exhibited lateral distensions.

Control osteoclasts possessed well-developed ruffled borders, whereas most of the BFA-treated osteoclasts showed poorly-formed ruffled borders (Fig. 2B). Furthermore, the number of vesicles and vacuoles in BFA-treated osteoclasts were somewhat reduced, compared with those of control osteoclasts. The ultrastructure of rER in the treated osteoclast was unaffected by BFA-administration. At a higher magnification, it became evident that the Golgi cisternae were not localized in an array. Instead, clusters of vesicular and tubular structures could be seen (Fig. 4B). Osteoclasts treated with WT exhibited no tendency to alter the ultrastructure of the Golgi apparatus, but were marked by the complete disappearance of ruffled borders, and a consequent increase in the number of vesicles and vacuoles in the cytoplasm (Figs. 3, 4C).

Localization of ACPase activity

The localization of ACPase, which is one of the lysosomal enzymes, was examined by enzyme cytochemical procedures. Under light microscopic observation, ACPase activity was detected primarily in the ruffled border adjacent to the bone matrix in control osteoclasts (Fig. 5A). In BFA-treated osteoclasts, ACPase activity, while somewhat reduced, was detected throughout the cytoplasm (Fig. 5B). Under TEM observation, reaction products of ACPase were observed in the vesicles, vacuoles and ruffled borders in control osteoclasts (Fig. 6A). BFA-treated osteoclasts also possessed ACPase-positive vesicles and tubular structures in the cytoplasm, but ACPase-positive ruffled borders were poorly developed or disappeared (Fig. 6B). In the Golgi area, ACPase activity was detected in the Golgi cisternae and peripheral vesicles in control osteoclasts (Fig. 4D). After BFA-administration, ACPase activity was still detectable in some of the vesicular and tubular structures in the Golgi regions (Fig. 4E). In WT-treated osteoclasts, ACPase-positive granular structures were localized throughout the cytoplasm under the light microscope (Fig. 5C). Under TEM observation, enzyme reaction products were located in many vesicles and vacuoles (Fig. 6C). These ACPase-positive vesicles and vacuoles were increased in number in WT-treated osteoclasts when compared with control osteoclasts. In the area of Golgi apparatus, the distribution of ACPase activity was the same as that of control osteoclasts (Fig. 4F).

Fig. 2. Transmission electron microscopic (TEM) images of the BFA-treated osteoclasts. **A:** Control osteoclast. The osteoclast reveals a well-developed ruffled border (RB) adjacent to the bone matrix (BONE). Golgi apparatus (Go) localize around each nucleus (N). Numerous vesicles and vacuoles (V) can be seen in the regions between the Golgi apparatus and ruffled border. The osteoclast possesses well-extended, but scattered rER (er) throughout the cytoplasm. **B:** BFA-treated osteoclast. The osteoclast lacks the ruffled border (arrowheads). The rER (er) is observed to be extended, as in the control. Original magnification = $\times 7000$, bar = 2 μm . CZ, clear zone; BONE, bone matrix; N, nucleus.

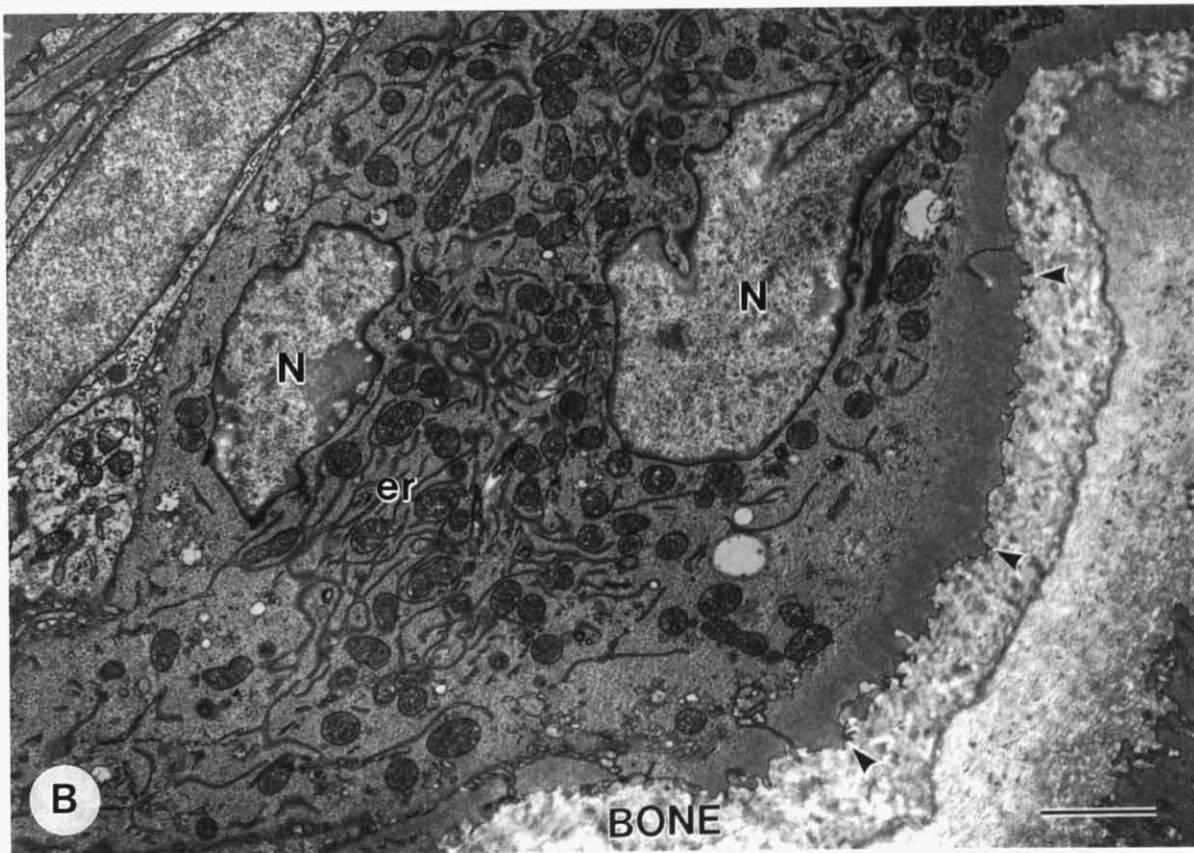
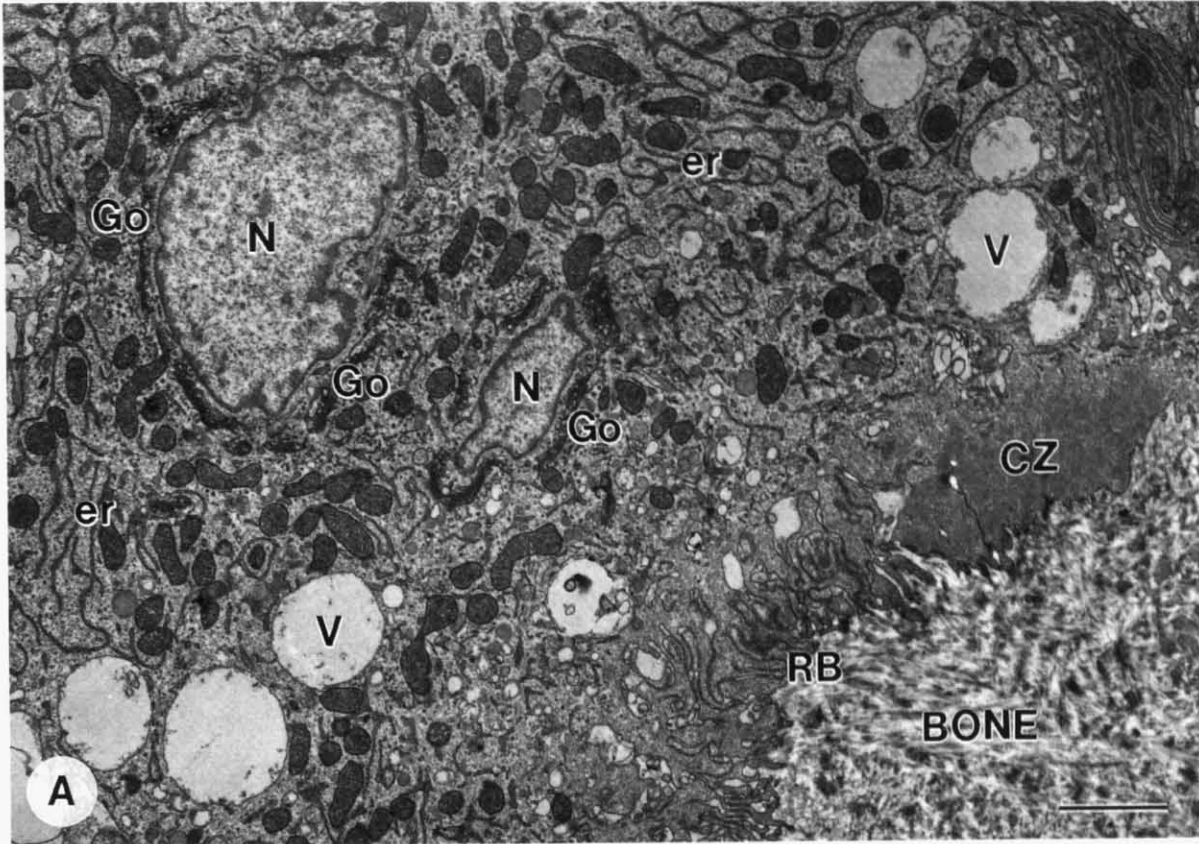


Fig. 2

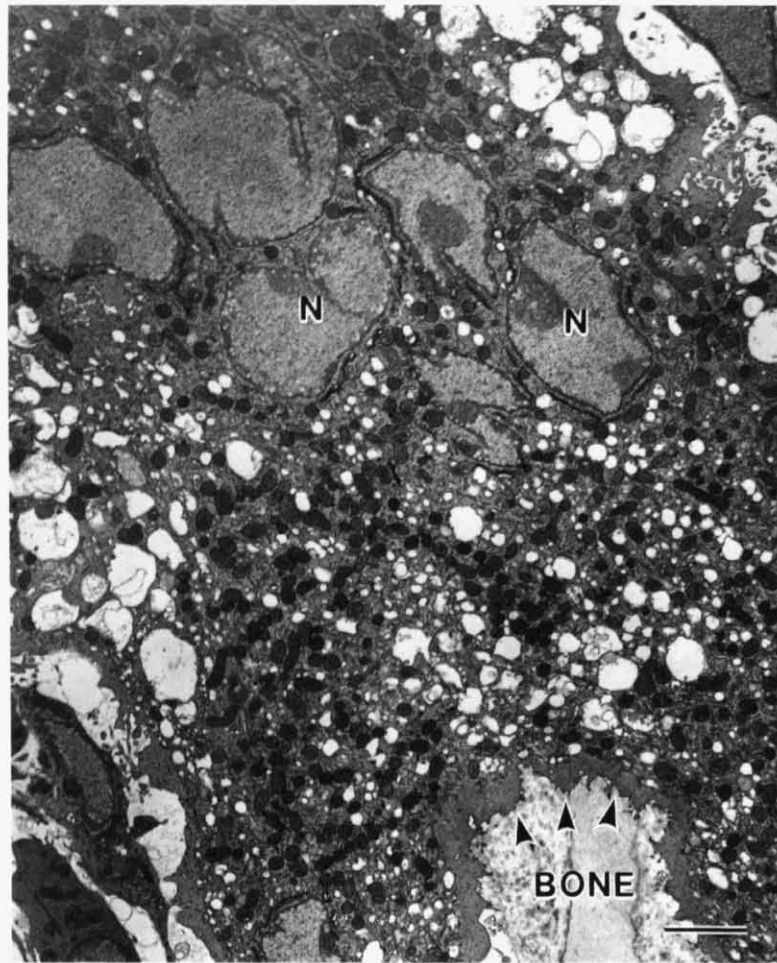


Fig. 3. TEM images of the WT-treated osteoclasts. The osteoclast is marked by the complete disappearance of ruffled borders (arrowheads), and a consequent increase in the number of vesicles and vacuoles in the cytoplasm. Original magnification = $\times 3500$, bar = $3 \mu\text{m}$. BONE, bone matrix; N, nucleus.

Localization of PNA-reaction

The relationship between Golgi apparatus and ruffled borders was examined by PNA cytochemistry. PNA reaction was localized mainly on the ruffled borders, as previously described [32, 45]. Under light microscopic observation, PNA-reactivity was intensely detected in the ruffled borders of control osteoclasts (Fig. 7A). After the administration of BFA, however, PNA cytochemistry revealed that treated-osteoclasts possessed few ruffled borders (Fig. 7B). Statistical analysis showed that 21.2% of BFA-treated osteoclasts had PNA-positive ruffled borders, whereas 71.5% of control osteoclasts possessed PNA-positive ruffled borders (Fig. 9). Under TEM observation, the ruffled border membrane reacted positively to PNA in the control osteoclast (Fig. 7C). Similar reactions were seen in the membranes of vacuoles located near the ruffled border. In BFA-treated osteoclasts, the number of PNA-positive ruffled border membranes and vacuoles was markedly reduced compared to that of control osteoclasts (Fig. 7D). On the other hand, PNA-reactivity in areas adjacent to the bone matrix completely disappeared in the

WT-treated osteoclasts (Fig. 8A). Only 0.8% of WT-treated osteoclasts possessed PNA-positive ruffled borders. Under TEM observation, PNA-reaction could be seen in the membranes of large vacuoles (Fig. 8B).

In a control, sections incubated without PNA displayed no reaction.

IV. Discussion

The molecular mechanism of BFA activity has been shown to inhibit the GTP-GDP exchange on the ADP-ribosylation factor (ARF), one of the small GTP-binding proteins, and subsequently blocks the binding of ARF to Golgi membranes [9, 19]. It has been reported that the ordinary structure of Golgi apparatus could not be identified anywhere, and the immunoreactivity for albumin was recognizable in the rER, the nuclear envelope, and small vesicles scattered to the cytoplasm in the rat hepatocytes treated with BFA [14]. Furthermore, Lippincott-Schwartz *et al.* [25] have demonstrated that BFA subsequently induced the formation of long tubulo-vesicular

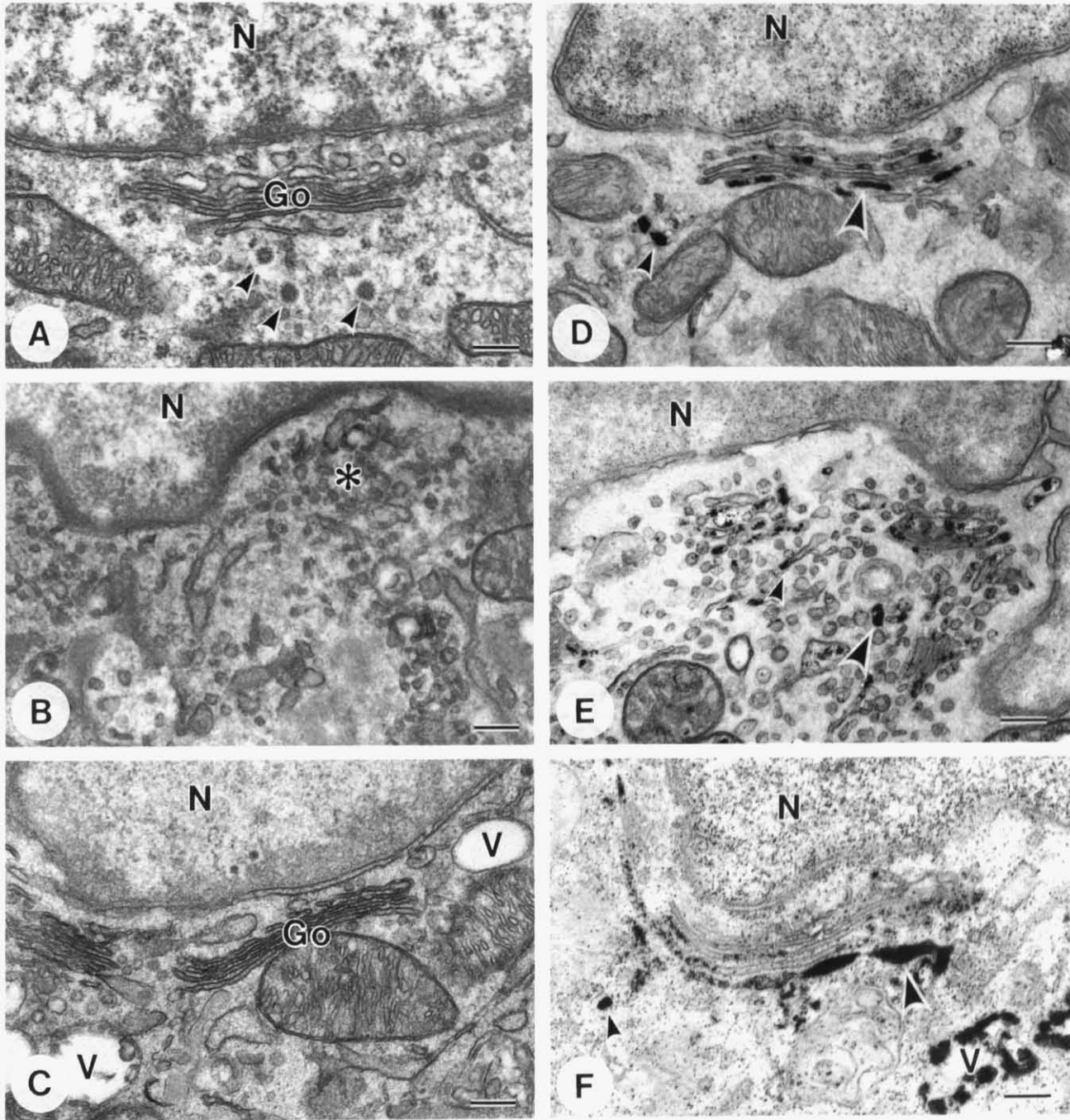


Fig. 4. TEM images of Golgi regions in osteoclasts. **A:** Control osteoclast. The Golgi apparatus consists of parallel arrays of several cisternae (Go) in the periphery of the nucleus and many vesicles (arrowheads) in the trans-face. **B:** BFA-treated osteoclast. The Golgi cisternae do not localize in an array, instead, the clusters of vesicular and tubular structures (*) are seen in the previous Golgi region. **C:** WT-treated osteoclast. The structure of Golgi apparatus is the same as that observed in the control. A vacuole (V) is positioned near the Golgi apparatus (Go). **D:** ACPase activity in control osteoclast. ACPase activity is detected in trans-cisternae (large arrowhead) and peripheral vesicles (small arrowhead). **E:** ACPase activity in BFA-treated osteoclast. ACPase activity is still observed in some vesicular (large arrowhead) and tubular structures (small arrowhead), in the previous Golgi regions. **F:** ACPase activity in WT-treated osteoclast. ACPase activity is detected in trans-cisternae (large arrowhead), peripheral vesicles (small arrowhead) and a vacuole (V). Original magnification = $\times 35000$, bar = $0.2 \mu\text{m}$. N: nucleus.

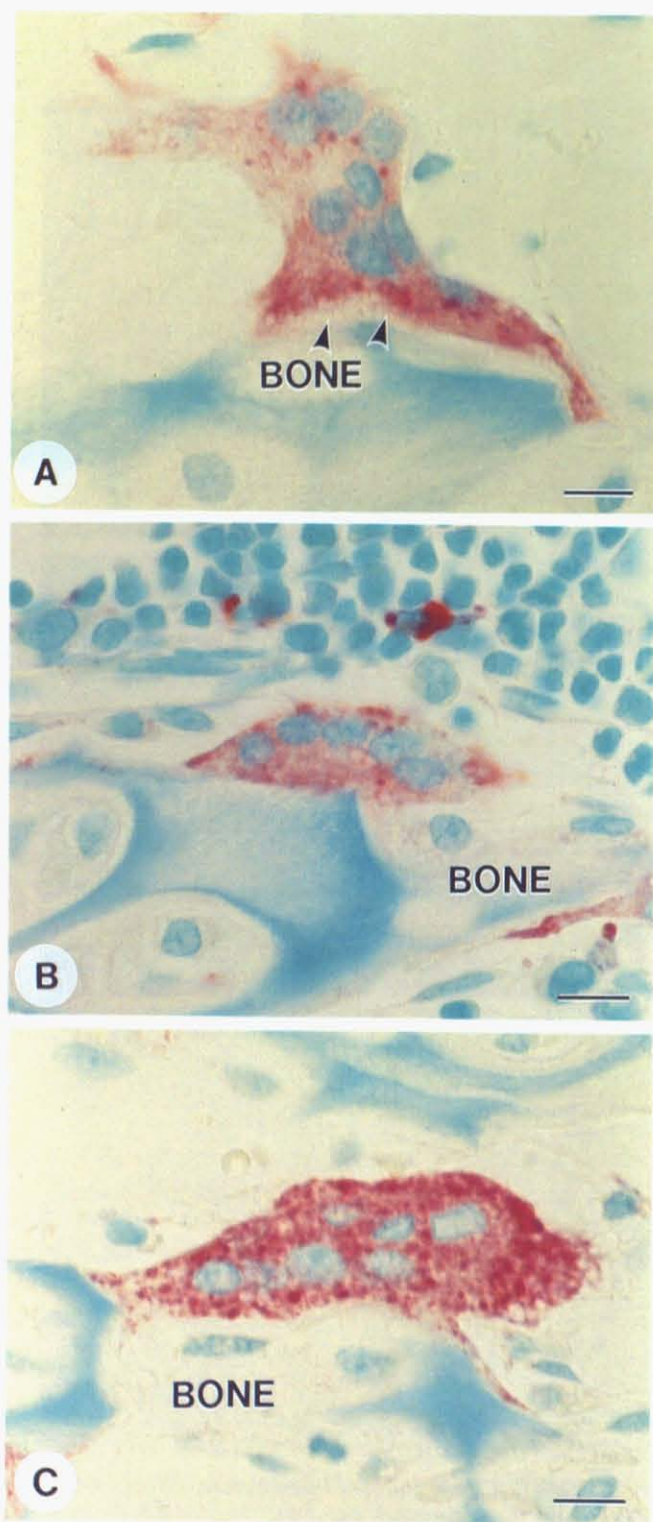


Fig. 5. Light microscopic images showing the localization of ACPase activity in osteoclasts. **A:** Light microscopic images of the control osteoclast. ACPase activity is detected primarily in the ruffled border (arrowheads) adjacent to the bone matrix (BONE). **B:** Light microscopic images of the BFA-treated osteoclast. ACPase activity is slightly detected throughout the cytoplasm. **C:** Light microscopic images of the WT-treated osteoclast. ACPase-positive granular structures are localized throughout the cytoplasm. Original magnification = $\times 500$, bar = $20 \mu\text{m}$. BONE: bone matrix.

processes extending from the Golgi apparatus to rER in a microtubule-dependent manner. Our TEM observations revealed the presence of vesicular and tubular structures in the Golgi region of osteoclasts treated with BFA, which may be consistent with the tubular processes reported by Lippincott-Schwartz *et al.* [25].

ACPase activity of normal osteoclasts localized in the Golgi cisternae, Golgi vesicles, vacuoles, ruffled borders and resorption lacunae gave rise to the idea that ACPase is secreted into the resorption lacunae, and sets about degrading the bone matrix proteins [28]. As regards the targeting of the lysosomal enzymes to the ruffled border, both cation-independent mannose-6-phosphate receptor (CI-M6PR), which recognizes lysosomal enzymes, and several lysosomal enzymes are co-localized in the Golgi apparatus and small transport vesicles. The localization of CI-M6PR on ruffled border membranes, and the presence of lysosomal enzymes under the ruffled border provides further support for the idea that Golgi-derived lysosomes are transported to the ruffled border, and subsequently secreted into the resorption lacunae [3]. This study showed the reduced formation of the ruffled borders positive for ACPase. These results lead to the postulation that the disruption of Golgi structures by BFA inhibits the transport of ACPase from Golgi apparatus to lysosomes and ruffled borders and reduces secretion of lysosomal enzymes into resorption lacunae. It has been reported that BFA exerted no inhibitory effect on the endocytotic pathway in cultured rat hepatocytes [31], and BFA appears to inhibit the vesicle-transport from Golgi apparatus to the ruffled border in the osteoclasts. Therefore, it seems likely that the inhibition of vesicular transport from Golgi apparatus results in the poor development of ruffled borders and reduced number of vesicles adjacent to the ruffled borders.

Ruffled borders of osteoclasts are regarded as a specific structure involved in the resorption of bone matrix [43]. Calcitonin (CT) is well-known to reduce the structure of ruffled borders of osteoclasts, consequently reducing activity of bone resorption [22]. In the experiment of radioautography using ^{125}I -elcatonin, developed silver grains of ^{125}I -elcatonin were located on plasma membranes of osteoclasts and were subsequently internalized. They accumulated especially in the Golgi apparatus, consequently making the Golgi apparatus smaller and irregularly-shaped with slightly-dispersed cisternae. It also induced the formation of many small vesicles in Golgi regions [21]. Furthermore, it has been reported that both thiamine pyrophosphatase [37] and ACPase activities [36] in the Golgi apparatus of CT-treated osteoclasts were lower than that in control osteoclasts. Thus, it is likely that the functional suppression of osteoclasts treated with CT, coincident with the disappearance of the ruffled borders, is closely associated with the disorganization of Golgi apparatus. Thus, cytological alterations of osteoclasts treated with CT were similar to those of the osteoclasts treated with BFA. However, Golgi cisternae of BFA-treated os-

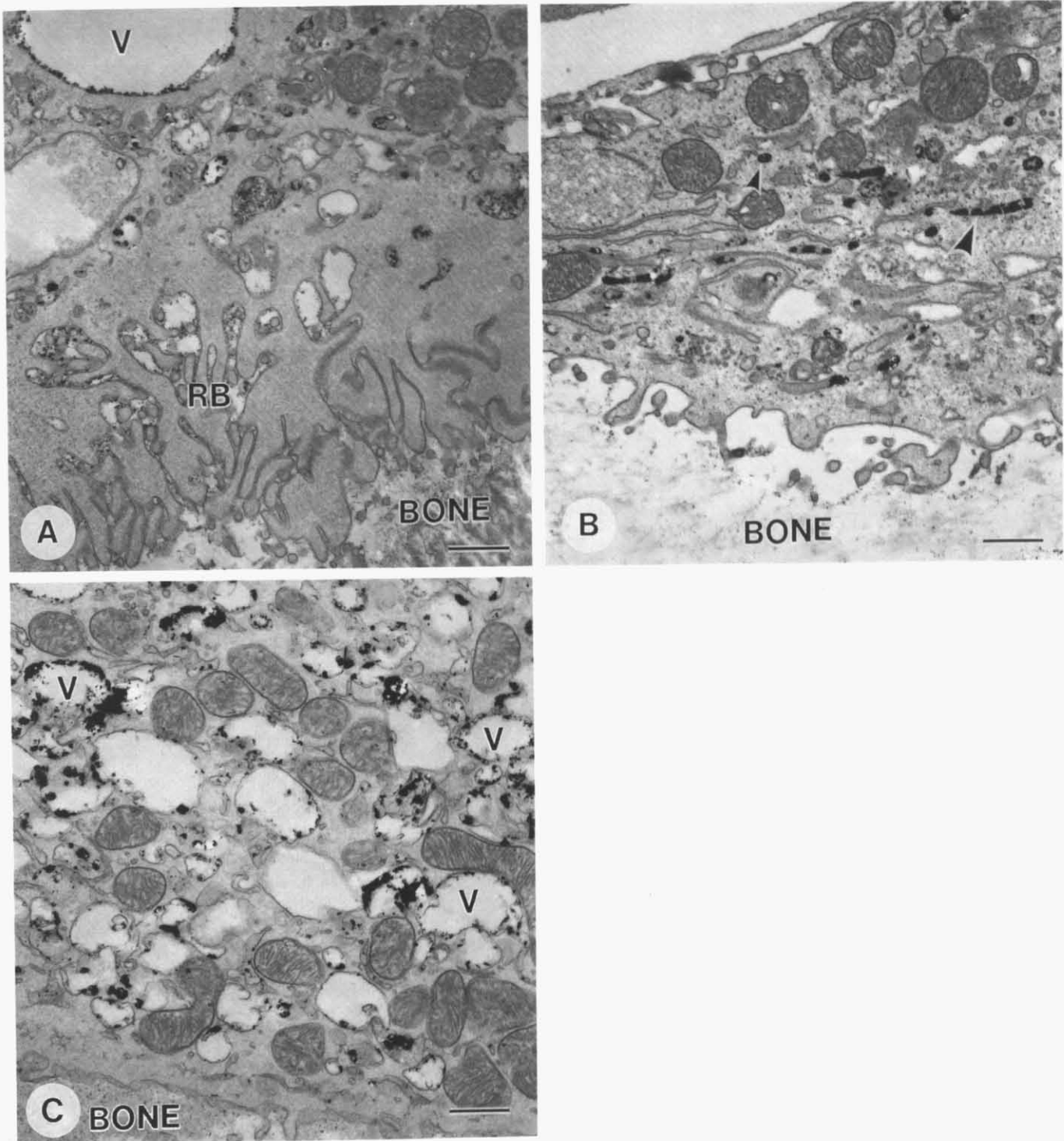


Fig. 6. TEM images showing the localization of ACPase activity in osteoclasts. **A:** TEM images of the control osteoclast. The localization of reaction products of ACPase is observed in the vesicles, vacuoles (V) and ruffled border (RB). **B:** TEM images of the BFA-treated osteoclast. Reaction products of enzyme are observed in the vesicles (small arrowhead) and tubular structures (large arrowhead). Note no ruffled border in this osteoclast. **C:** TEM images of the WT-treated osteoclast. The enzyme reaction products are seen in many vesicles and vacuoles (V). Original magnification = $\times 20000$, bar = $0.5 \mu\text{m}$. BONE: bone matrix.

teoclasts were vesiculated more severely than those of CT-treated osteoclasts. To elucidate the relationship between Golgi apparatus and ruffled borders of osteoclasts, we observed the PNA-reaction that recognized ruffled border

membranes. In the BFA-treated osteoclasts, PNA-positive ruffled borders were seldom observed. Thus, the dissociation of Golgi apparatus and the simultaneous disappearance of the ruffled border supports the postu-

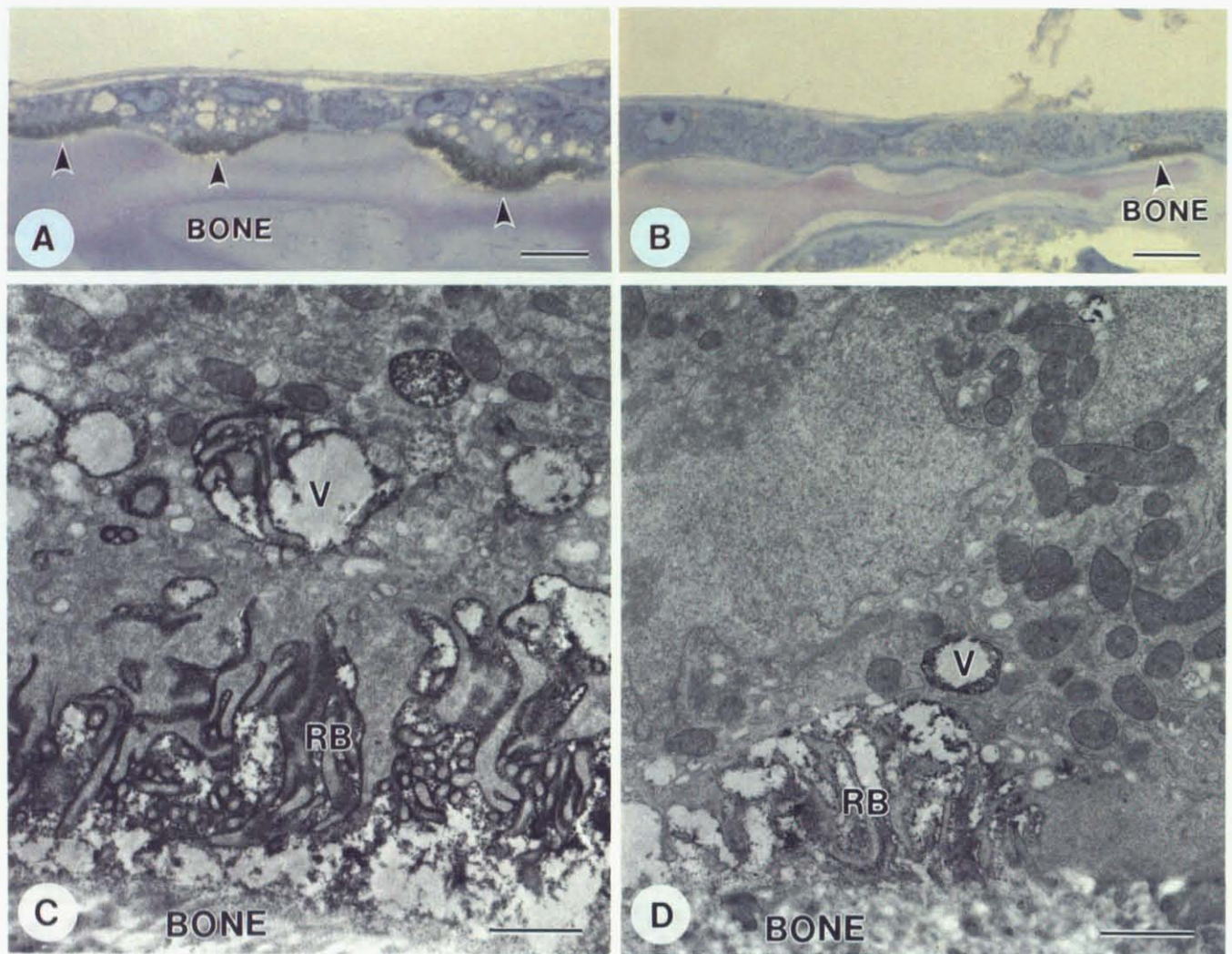


Fig. 7. PNA-reactivity localization in BFA-treated osteoclasts. **A:** Light microscopic images of the control osteoclast. Intense PNA reaction is detected on the ruffled borders (arrowheads) of osteoclasts adjacent to the bone-matrix (BONE). **B:** Light microscopic images of the BFA-treated osteoclast. A mild reaction to PNA (arrowhead) is observed in osteoclasts adjacent to the bone matrix (BONE). **C:** TEM images of the control osteoclast. Intense PNA reactivity is detected on the ruffled border membrane (RB) and vacuoles (V) adjacent to the bone matrix (BONE). **D:** TEM images of the BFA-treated osteoclast. The number of PNA-positive ruffled border membranes (RB) and vacuoles (V) is reduced, compared with that seen in control osteoclasts. **A, B:** Original magnification = $\times 1000$, bar = $10 \mu\text{m}$. **C, D:** Original magnification = $\times 14000$, bar = $1 \mu\text{m}$. BONE: bone matrix.

lation that Golgi apparatus plays an important role in vesicle and membrane targeting to the ruffled border. It has been reported that BFA blocked constitutive secretion of glycosaminoglycan chains, that had been synthesized and sulfated in the trans-Golgi cisternae of BHK-21 cells, and inhibited granule formation of secretogranin II from the TGN in PC12 cells, suggesting that BFA inhibited transport not only from the rER to the Golgi apparatus, but also from the distal Golgi compartments, including TGN, towards the cell-surface via both the constitutive and the regulated pathways [30]. It has also been described that BFA blocks the formation of constitutive secretory vesicles and immature secretory granules from the TGN in PC12 cells [42]. Similar to the inhibition of vesicle-targeting to the cell-surfaces seen in other cells,

our study indicates that BFA caused a disruption of vesicular transport from Golgi apparatus toward the ruffled borders of osteoclasts.

On the other hand, it has been reported that osteoclasts express high levels of pp60^{c-src} [20, 46], targeted disruption of *c-src* in mice induce osteopetrosis [44] and these osteoclasts lack ruffled borders [5]. PI3-kinase is one of the enzymes that may be activated by the *c-src* tyrosine kinase [10, 11]. It has been shown that WT, a specific inhibitor of PI3-kinase, causes the disappearance of ruffled borders of osteoclasts [34, 35] and subsequently inhibits bone resorption [18, 35]. In our study, WT-treated osteoclasts were also marked by the complete disappearance of ruffled borders, and a consequent increase in the number of vesicles and vacuoles in the cytoplasm,

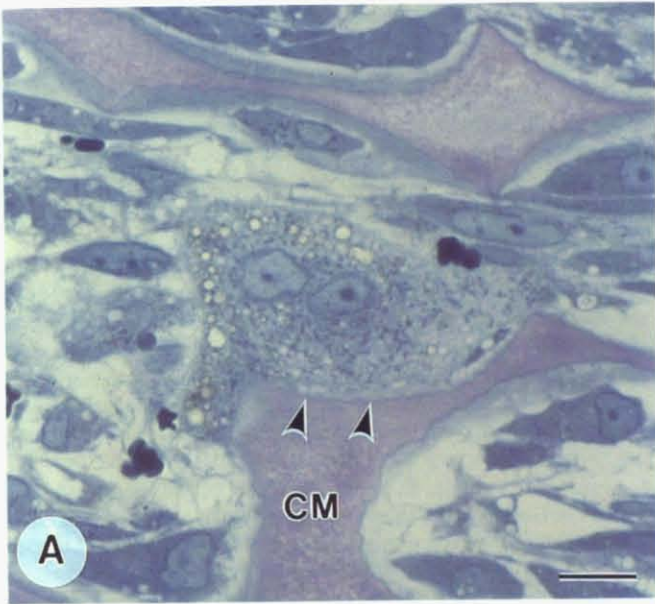


Fig. 8. The localization of PNA-reactivity in WT-treated osteoclasts. **A:** Light microscopic images of the WT-treated osteoclast. No PNA-reaction (arrowheads) is observed adjacent to the cartilage matrix (CM). **B:** TEM images of the WT-treated osteoclast. PNA-positive ruffled border membranes disappear (arrowheads) and a lot of PNA-positive large vacuoles (V) are observed in the cytoplasm. **A:** Original magnification = $\times 1000$, bar = $10 \mu\text{m}$. **B:** Original magnification = $\times 14000$, bar = $1 \mu\text{m}$. CM: cartilage matrix.

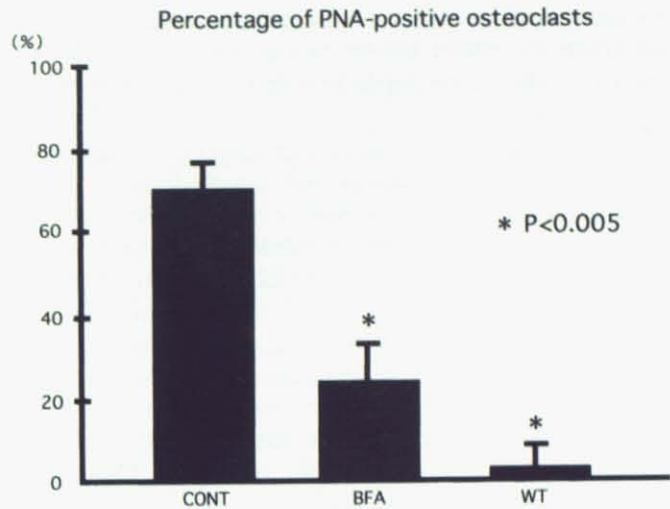


Fig. 9. Statistical analysis of osteoclasts which possess PNA-positive ruffled borders. 71.5 ± 7.1% of osteoclasts possessed PNA-positive ruffled borders in the control experiments (CONT). In contrast, BFA-, and WT-treatment reduced the numbers of PNA-positive osteoclasts to 21.2 ± 11.3% and 0.8 ± 1.8%, respectively.

but the Golgi apparatus showed no ultrastructural and cytochemical changes. CT-treated osteoclasts also lost the ruffled borders, but the number of cytoplasmic vesicles and vacuoles of WT-treated osteoclasts was more than that of CT-treated osteoclasts. These results indicate that the structures and functions of the Golgi apparatus of osteoclasts are not affected by WT. From the standpoint of morphology, PI3-kinase would appear to be involved in the regulation of post-Golgi membrane transport of osteoclasts.

It has been reported that WT-treated K-562 cells induced secretion of procathepsin D with inhibition of accurate targeting to lysosomes [8]. Moreover, Brown *et al.* [6] have shown that WT causes a highly specific dilation of M6PR-enriched vesicles of the prelysosomal compartment in several cell lines, suggesting that PI3-kinase regulates the trafficking of lysosomal enzymes by interfering with a M6PR-dependent sorting event in the TGN. It seems likely, therefore, that the intracellular accumulation of ACPase-positive vesicles and vacuoles in WT-treated osteoclasts result from the inhibition of the transport and the secretion of lysosomal enzymes from ruffled borders to resorption lacunae which are considered to be the functional equivalent of secondary lysosomes [1].

Nakamura *et al.* [34] have demonstrated that WT causes the disappearance of ruffled borders and the accumulation of vacuoles containing vacuolar H^+ -ATPase in osteoclast-like multinucleated cells (OCLs) formed *in vitro*, suggesting that PI3-kinase plays an important role in ruffled border formation in osteoclasts, probably in fusion of membrane vacuoles with the plasma membrane. In this study, WT-treated osteoclasts were also marked by both the disappearance of ruffled borders and consequent increase of PNA-positive large vacuoles. Ruffled borders

are recognized by PNA, so these large vacuoles seem to be the result of ruffled border precursors fusing with one another in the cytoplasm and/or endocytosed membranes of ruffled borders.

In summary, BFA-treated osteoclasts were marked by dissociated Golgi apparatus and poorly-formed ruffled borders. Also the ACPase activity was somewhat reduced when compared with control osteoclasts. These results indicate that the maintenance of Golgi structures of osteoclasts plays an important role in both the formation of lysosomal enzymes and supply of ruffled border membranes. Furthermore, WT-treated osteoclasts, although bearing no signs of ultrastructural alteration of Golgi apparatus, were marked by the complete obliteration of ruffled borders, and a consequent increase in the number of PNA-positive vacuoles, suggesting that PI 3-kinase is involved in the transport of lysosomal enzymes and the maintenance of ruffled borders.

V. Acknowledgments

This work was supported, in part, by a grant from Research Fellowships of the Japan Society for the Promotion of Science for Young Scientists (N. I), Uehara Memorial Foundation (N. A) and a Grant-in-aid from the Ministry of Education, Science, and Culture of Japan (N. A). We also wish to thank Mr. Kendall J. T. Walls for his invaluable assistance in the preparation of the manuscript.

VI. References

- Baron, R., Neff, L., Louvard, D. and Courtoy, P. J.: Cell-mediated extracellular acidification and bone resorption: evidence for a low pH in resorbing lacunae and localization of a 100-kD lysosomal membrane protein at the osteoclast ruffled border. *J. Cell Biol.* 101; 2210–2222, 1985.
- Baron, R., Neff, L., Brown, W., Louvard, D. and Courtoy, P. J.: Selective internalization of the apical plasma membrane and rapid redistribution of lysosomal enzymes and mannose-6-phosphate receptors during osteoclast inactivation by calcitonin. *J. Cell Sci.* 97; 439–447, 1990.
- Baron, R., Neff, L., Brown, W., Courtoy, P. J., Louvard, D. and Farquhar, M. G.: Polarized secretion of lysosomal enzymes: co-distribution of cation-independent mannose-6-phosphate receptors and lysosomal enzymes along the osteoclast exocytic pathway. *J. Cell Biol.* 106; 1863–1872, 1988.
- Blair, H. C., Teitelbaum, S. L., Chiselli, R. and Gluck, S.: Osteoclastic bone resorption by a polarized vacuolar proton pump. *Science* 245; 855–857, 1989.
- Boyce, B. F., Yoneda, Y., Lowe, C., Soriano, P. and Mundy, G. R.: Requirement of pp60^{c-src} expression for osteoclasts to form ruffled borders and resorb bone in mice. *J. Clin. Invest.* 90; 1622–1627, 1992.
- Brown, W. J., DeWald, D. B., Emr, S. D., Plutner, H. and Balch, W. E.: Role for phosphatidylinositol 3-kinase in sorting and transport of newly synthesized lysosome enzymes in mammalian cells. *J. Cell Biol.* 130; 781–796, 1995.
- Cameron, D. A.: The Golgi apparatus in bone and cartilage cells. *Clin. Orthop.* 58; 191–211, 1968.
- Davidson, H. W.: Wortmannin causes mistargeting of procathepsin D. Evidence for the involvement of a phosphatidylinositol 3-kinase in vesicular transport to lysosomes. *J. Cell Biol.* 130; 797–805, 1995.
- Donaldson, J. G., Finazzi, D. and Klausner, R. D.: Brefeldin A inhibits Golgi membrane-catalysed exchange of guanine nucleotide onto ARF protein. *Nature* 360; 350–352, 1992.
- Fukui, Y. and Hanafusa, H.: Phosphatidylinositol kinase activity associates with viral p60src protein. *Mol. Cell Biol.* 9; 1651–1658, 1989.
- Fukui, Y., Kornbluth, S., Jong, S. M., Wang, L. H. and Hanafusa, H.: Phosphatidylinositol kinase type I activity associates with various oncogene products. *Oncogene Res.* 4; 283–292, 1989.
- Fujita, H. and Okamoto, H.: Fine structural localization of thiamine pyrophosphatase and acid phosphatase activities in the mouse pancreatic acinar cell. *Histochemistry* 64; 287–295, 1979.
- Fujiwara, T., Oda, K. and Ikehara, Y.: Dynamic distribution of the Golgi marker thiamine pyrophosphatase is modulated by brefeldin A in rat hepatoma cells. *Cell Struct. Funct.* 14; 605–616, 1989.
- Fujiwara, T., Oda, K., Yokota, S., Takasaki, A. and Ikehara, Y.: Brefeldin A causes disassembly of the Golgi complex and accumulation of secretory proteins in the endoplasmic reticulum. *J. Biol. Chem.* 263; 18545–18552, 1988.
- Gomori, G.: *Microscopic Histochemistry, Principle and Practice*, University of Chicago Press, Chicago, 1952, pp. 189.
- Goto, T., Kiyoshima, T., Morii, R., Tsukuba, T., Nishimura, Y., Himeno, M., Yamamoto, K. and Tanaka, T.: Localization of cathepsins B, D, and L in the rat osteoclast by immuno-light and electron microscopy. *Histochemistry* 101; 33–40, 1994.
- Griffith, G. and Simons, K.: The trans Golgi network: sorting at the exit site of the Golgi complex. *Science* 234; 438–443, 1986.
- Hall, T. J., Jeker, H. and Schaubelin, M.: Wortmannin, a potent inhibitor of phosphatidylinositol 3-kinase, inhibits osteoclastic bone resorption in vitro. *Calcif. Tissue Int.* 56; 336–338, 1995.
- Helms, J. D. and Rothman, J. E.: Inhibition by brefeldin A of a Golgi membrane enzyme that catalyses exchanges of guanine nucleotide bound to ARF. *Nature* 360; 350–352, 1992.
- Horne, W. C., Neff, D., Chatterjee, D., Lomri, A., Levy, J. B. and Baron, R.: Osteoclasts express high levels of pp60^{c-src} in association with intracellular membranes. *J. Cell Biol.* 119; 1003–1013, 1992.
- Ikegame, M., Ejiri, S. and Ozawa, H.: Histochemical and Autoradiographic studies on calcitonin internalization and intracellular movement in osteoclasts. *J. Bone Miner. Res.* 9; 25–37, 1994.
- Kallio, D. M., Garant, P. R. and Minkin, C.: Ultrastructural effects of calcitonin on osteoclasts in tissue culture. *J. Ultrastruct. Res.* 39; 205–216, 1972.
- Kaneko, H., Sasaki, T., Ramamurthy, N. S. and Golub, L. M.: Tetracycline administration normalizes the structure and acid phosphatase activity of osteoclasts in streptozotocin-induced diabetic rats. *Anat. Rec.* 227; 427–436, 1990.
- Lippincott-Schwartz, J., Yuan, L. C., Bonifacino, J. S. and Klausner, R. D.: Rapid redistribution of Golgi proteins into the ER in cells treated with brefeldin A: evidence for membrane cycling from Golgi to ER. *Cell* 56; 801–813, 1989.
- Lippincott-Schwartz, J., Donaldson, J. G., Schweizer, A., Berger, E. G., Hauri, H.-P., Yuan, L. C. and Klausner, R. D.: Microtubule-dependent retrograde transport of proteins into the ER in the presence of brefeldin A suggests an ER recycling pathway. *Cell* 60; 821–836, 1990.
- Littlewood-Evans, A., Kokubo, T., Ishibashi, O., Inaoka, T.,

- Wlodarski, B., Gallagher, J. A. and Bilbe, G.: Localization of cathepsin K in human osteoclasts by in situ hybridization and immunohistochemistry. *Bone* 20; 81–86, 1997.
27. Lotan, R., Skutelsky, E., Danon, D. and Sharon, N.: The purification, composition, and specificity of anti-T lectin from peanut (*Arachis hypogaea*). *J. Biol. Chem.* 250; 8518–8523, 1975.
28. Lucht, U.: Acid phosphatase of osteoclasts demonstrated by electron microscopic histochemistry. *Histochemie* 28; 103–117, 1971.
29. Miller, S. C.: The rapid appearance of acid phosphatase activity at the developing ruffled border of parathyroid hormone activated medullary bone osteoclasts. *Calcif. Tissue Int.* 37; 526–529, 1985.
30. Miller, S. G., Carnel, L. and Moore, H-P.H.: Post-Golgi membrane traffic: brefeldin A inhibits export from distal Golgi compartments to the cell surface but not recycling. *J. Cell Biol.* 118; 267–283, 1992.
31. Misumi, Yo., Misumi, Yu., Miki, K., Takasaki, A., Tamura, G. and Ikehara, Y.: Novel blockade by brefeldin A of intracellular transport of secretory proteins in cultured rat hepatocytes. *J. Biol. Chem.* 261; 11398–11403, 1986.
32. Nakamura, H. and Ozawa, H.: Characteristic localization of carbohydrates in osteoclasts by lectin cytochemistry. *Bone* 13; 411–416, 1992.
33. Nakamura, H., Moriyama, Y., Futani, M. and Ozawa, H.: Immunohistochemical localization of vacuolar H⁺-ATPase in osteoclasts of rat tibiae. *Arch. Histol. Cytol.* 57; 535–539, 1994.
34. Nakamura, I., Sasaki, T., Tanaka, S., Takahashi, N., Jimi, E., Kurokawa, T., Kita, Y., Ihara, S., Suda, T. and Fukui, Y.: Phosphatidylinositol-3 kinase is involved in ruffled border formation in osteoclasts. *J. Cell. Physiol.* 172; 230–239, 1997.
35. Nakamura, I., Takahashi, N., Sasaki, T., Tanaka, S., Udagawa, N., Murakami, H., Kimura, K., Kabuyama, Y., Kurokawa, T., Suda, T. and Fukui, Y.: Wortmannin, a specific inhibitor of phosphatidylinositol-3 kinase, blocks osteoclastic bone resorption. *FEBS Lett.* 361; 79–84, 1995.
36. Noda, K., Nakamura, Y. and Kuwahara, Y.: Histochemical studies of lysosomal forming system in osteoclasts with calcitonin treatment: acid phosphatase and glucose-6-phosphate. *Acta Histochem. Cytochem.* 30; 173–179, 1997.
37. Noda, K., Nakamura, Y., Wakimoto, Y., Tanaka, T. and Kuwahara, Y.: Thiamine pyrophosphatase activity in the Golgi apparatus of calcitonin-treated osteoclasts. *J. Electron Microsc.* 40; 399–402, 1991.
38. Oda, K., Hirose, S., Takami, N., Misumi, Y., Takasaki, A. and Ikehara, Y.: Brefeldin A arrests the intracellular transport of a precursor of complement C3 before its conversion site in rat hepatocytes. *FEBS Lett.* 214; 135–138, 1987.
39. Oguro, I. and Ozawa, H.: Cytochemical studies of the cellular evidents sequence in bone remodeling: Cytological evidence for a coupling mechanism. *J. Bone Miner. Metab.* 7; 30–36, 1989.
40. Okada, T., Sakuma, L., Fukui, Y., Hazeki, O. and Ui, M.: Blockage of chemotactic peptide-induced stimulation of neutrophils by wortmannin as a result of selective inhibition of phosphatidylinositol 3-kinase. *J. Biol. Chem.* 269; 3563–3567, 1994.
41. Reponen, P., Sahlberg, C., Munant, C., Thesleff, I. and Tryggvason, K.: High expression of 92-kD Type IV collagenase (gelatinase B) in the osteoclast lineage during mouse development. *J. Cell Biol.* 124; 1091–1102, 1994.
42. Rosa, P., Barr, F. A., Stinchcombe, J. C., Binacchi, C. and Huttner, W. B.: Brefeldin A inhibits the formation of constitutive secretory vesicles and immature secretory granules from the trans-Golgi network. *Eur. J. Cell Biol.* 59; 265–274, 1992.
43. Scott, B. L. and Pease, D. C.: Electron microscopy of the epiphyseal apparatus. *Anat. Rec.* 126; 465–495, 1956.
44. Soriano, P., Montgomery, C., Geske, R. and Bradley, A.: Target disruption of the c-src proto-oncogene leads to osteopetrosis in mice. *Cell* 64; 693–702, 1991.
45. Takagi, M., Yagasaki, H., Baba, T. and Baba, H.: Ultrastructural visualization of selective peanut agglutinin binding sites in rat osteoclasts. *J. Histochem. Cytochem.* 36; 95–101, 1988.
46. Tanaka, S., Takahashi, N., Udagawa, N., Sasaki, T., Fukui, Y., Kurokawa, T. and Suda, T.: Osteoclasts express high levels of p60^{c-src}, preferentially on ruffled border membranes. *FEBS Lett.* 313; 85–89, 1992.
47. Tezuka, K., Nemoto, K., Tezuka, Y., Sato, T., Ikeda, Y., Kobori, M., Kawashima, H., Eguchi, H., Hakeda, Y. and Kumegawa, M.: Identification of matrix metalloproteinase 9 in rabbit osteoclasts. *J. Biol. Chem.* 269; 15006–15009, 1994.
48. Toki, C., Fujiwara, T., Sohda, M., Hong, H-S., Misumi, Y. and Ikehara, Y.: Identification and characterization of rat 364-kDa Golgi-associated protein recognized by autoantibodies from a patient with rheumatoid arthritis. *Cell Struct. Funct.* 22; 565–577, 1997.
49. Yano, H., Nakanishi, S., Kimura, K., Hanai, N., Saitoh, Y., Fukui, Y., Nonomura, Y. and Matsuda, Y.: Inhibition of histamine secretion by wortmannin through the blockade of phosphatidylinositol 3-kinase in RBL-2H3 cells. *J. Biol. Chem.* 268; 25846–25856, 1993.